Design and simulation of Cd1-xZnxTe thin films epitaxied on CdTe substrate for photovoltaic devices applications

A. Aissat, M. Fathi, Jean-Pierre Vilcot

Available online at www.sciencedirect.com

ScienceDirect

Energy Procedia 36 (2013) 86 – 93

Energy Procedia

TerraGreen 13 International Conference 2013 - Advancements in Renewable Energy and Clean Environment

Design and simulation of $Cd_{1-x}Zn_xTe$ thin films epitaxied on CdTe substrate for photovoltaic devices applications

A. Aissat [a]*, M. Fathi[b], and J.P. Vilcot[c]

[a] *LATSI Laboratory, Faculty of the Engineering Sciences, university Saad Dahlab Blida, BP270, 09.000, Algeria*
[b] *CRTSE Semiconductor Technology Research Center for Energetics, B.P.140 Alger Sept Merveilles, 16027 Algiers, Algeria*
[c] *Institut d'Electronique, de Microélectronique et de Nanotechnologie (IEMN), UMR CNRS 8520, Université des Sciences et Technologies de Lille 1, Avenue Poincarré, BP 60069, 59652 Villeneuve d'Ascq, France*

Abstract

This work concerns the study and the simulation of a structure containing II-VI semiconductor for photovoltaic application. We studied the influence of the zinc concentration on the various parameters of the alloy $Cd_{1-x}Zn_xTe$ epitaxied on a CdTe substrate. Indeed, the insertion of zinc increases the band gap of the alloy, which is not ideal to absorb the maximum of the solar spectrum, but for low concentrations of zinc the $Cd_{1-x}Zn_xTe$ ternary material becomes attractive in the photovoltaic field. We have shown that for a Zinc composition (x) = 5%, the band gap is 1.52eV. And if x = 20%, the gap is 1.62eV.Our simulation studies have demonstrated that by an introduction of a specific Zinc concentration, we successfully simulated the achieving of 19% efficiency for solar devices.

Keywords: semiconductors, solar cell,optoelectronics;

1. Introduction

Photovoltaic solar energy is a big part in the research, and is growing increasingly important since 1990.This research his focused on two main areas, which may seem opposites (increased cell efficiency and lower cost of production) [1,2]. This development essentially involves mastering of materials used in the design of components. Most of these materials are obtained by standard alloy substrates. They could in principle cover a wide range of compositions and there fore applications [3].The alloys of CdTe subject of this work provide attractive performances for the development of solar cells and can be competitive to silicon and III-V compounds. Binary and ternary compounds based on II-VI semiconductor present very important features that allow them to be competitive candidates to silicon and III-V compounds for photovoltaics and optoelectronics in the visible. They form a class of materials whose gap ranges from 3.84eV (ZnS) to 1.5 eV (CdTe) at room temperature. Their appeal lies in their strong absorption coefficient and wide band gap and their low production costs [4]. In our study we are interested primarily based compounds of cadmium telluride and will be used for our structure. The interest in these compounds is further enhanced by the possibility of making alloys by combination of elements belonging to these columns II and VI. This gives the ternary alloy type $Cd_{1-x}Zn_xTe$.

* Corresponding author.
E-mail address:sakre23@yahoo.fr

doi:10.1016/j.egypro.2013.07.011

Nomenclature

q electron charge

V voltage across the junction

K Boltzmann constant

Φ flux of incident illumination

T temperature (K)

A Area of the PV cell

J_{ph} generated photo-current density

J_{Te} thermionic current density

J_{dif} diffusion current density

Δ_0 Energy bands shift of spin-spitted holes.

E_{hh} Energy Band of the heavy hole.

E_{lh} Energy Band of the light hole.

2. Theoretical approach

II-VI Semiconductors crystallize in the cubic structure; Zinc blend structure precisely, also called sphalerite. The mesh of this structure is composed of two face-centered cubic lattices, offset by a quarter of the diagonal of the cube of the [5]. The lattice parameter depends on the nature of the chemicals put into play crystal lattice is much greater than the atomic number of component parts is large. The lattice parameter of an alloy $A_{(1-x)}B_xC$ is calculated by the Vegard's law given by:

$$a_{CdZnTe} = x a_{ZnTe} + (1 - x) a_{CdTe} \quad (1)$$

The principal of “strained layer” and “critical thickness”.

2.1.1 The Strain.

During the epitaxial growth, there is the problem of stresses due to lattice mismatch between the deposited layer and the substrate. Epitaxial layers grow out of pseudo morphicinitially before relaxing plastically or elastically. Indeed, in a pseudo morphic growth on a standard substrate, the substrate is too thick to be able to deform significantly, the mesh layer epitaxial growth therefore complies in the surface plane, them substrate $a_{//} = a_s$ deforms elastically and consequently in the direction perpendicular $a_{\perp}$ claimed that the lattice parameter of the layer is smaller or larger than that of the substrate deformation layer is either an elongation intension "either shrinkage" compression layer [6]. For a description of the effect of strain on the band structure we used the model and Van Walle and used formalism Krijin [7].Both parallel and perpendicular components of the tensor of the deformation can be defined as follows:

$$\mathcal{E}_{\parallel} = \frac{a_{\parallel} - a}{a} \tag{2}$$

$$\mathcal{E}_{\perp} = \frac{a_{\perp} - a}{a} \tag{3}$$

For a to tally strained layer:

$$a_{\parallel} = a_{sub} \tag{4}$$

$$\mathcal{E}_{\perp} = -2 \times \frac{C_{12}}{C_{11}} \times \mathcal{E}_{\parallel} \tag{5}$$

In the absence of stress, the heavy holes band and light hole are degenerated and isotropic in the center of the Brillouin zone, and the spin-band holes are located at energy Δ_0 below the two bands. The center of gravity of the valence band average energy $E_{V,moy}$ is there fore $\frac{\Delta_0}{3}$ below the top of the valence band at k =0.

$$E_{V,moy} = \frac{E_{HH} + E_{LH} + \Delta_0}{3} \tag{6}$$

E_{HH}: energy band of the heavy hole.
E_{LH}: energy band of the light hole.
Δ_0: energy bands shift of spin-spitted holes.

The strain effect on the valence and conduction bands could be decomposed into two parts:

- The hydrostatic component, linked to the deformation along the axis of growth, causes a shift of the center of gravity of the valence band and the center of gravity of the conduction band.
- The shear stress, lift the degeneracy of energy states of heavy holes and light hole in $k = 0$ (typically a value Δ_{hh-lh} of the order of 60-80meV for a lattice mismatch of 1% [7]).

For an epitaxial layer subject to strain biaxial compression, the hydrostatic component increases the gap between the valence band and the conduction band, and the shear stress makes the valence bands strongly anisotropic[7], the band higher energy becomes heavy as $k_{\perp}$ and light according $k_{\parallel}$ (HH band). The lower energy band becomes lightly as $k_{\perp}$ and heavy as $k_{\parallel}$ (LH band). Energy shifts of the centers of gravity of the valence band and the conduction band K= 0 induced by hydrostatic stress, vary proportionally to the strain [7]:

$$\Delta E_{V,moy}^{hyd} = a_v(2\mathcal{E}_{\parallel} + \mathcal{E}_{\perp}) \tag{7}$$

$$\Delta E_{c}^{hyd} = a_c(2\mathcal{E}_{\parallel} + \mathcal{E}_{\perp}) \tag{8}$$

With $a_c and\ a_v$potentials hydrostatic deformation due to the conduction band and the valence band, respectively. Energy shift induced by the shear stressing each of the strips forming the valence band are, in the case of a growth substrate. [8]

$$\Delta\ E_{hh}^{cisa} = -\frac{1}{2} \times \delta E^{cisa} \tag{9}$$

$$\Delta E_{lh}^{cisa} = -\frac{1}{2}\Delta_0 + \frac{1}{4}\delta E^{cisa} + \frac{1}{2}.\sqrt{\Delta_0^2 + \Delta_0\,\delta E^{cisa} + \frac{9}{4}(\delta E^{cisa})^2} \quad (10)$$

$$\Delta E_{so}^{cisa} = -\frac{1}{2}\Delta_0 + \frac{1}{4}\delta E^{cisa} - \frac{1}{2}.\sqrt{\Delta_0^2 + \Delta_0\,\delta E^{cisa} + \frac{9}{4}(\delta E^{cisa})^2} \quad (11)$$

with:

$$\delta E^{cisa,100} = 2.b.(\varepsilon_{\parallel} + \varepsilon_{\perp}) \quad (12)$$

Where b is the tetragonal deformation potential.

Taking as reference energy $E_{v,moy}$ (equation 6), and taking into account equations (7), (8), (9), (10), we can define the energy of the top of the valence band and the energy of the bottom of the conduction band.

E_v: Energy from the top of the valence band is:

$$E_v = E_{v,moy} + \frac{\Delta_0}{3} + \Delta E_{v,moy}^{hyd} + max\left(\Delta E_{hh}^{cisa}, \Delta E_{lh}^{cisa}\right) \quad (13)$$

E_c: The energy of the bottom of the conduction band is:

$$E_c = E_{v,moy} + \frac{\Delta_0}{3} + E_g + \Delta E_c^{hyd} \quad (14)$$

In these expressions $E_{v,moy}$, the spin-orbit bursting $\Delta_0$and Energy gap are related to the unstrained material. From equations (13) and (14) we can determine the equation of strained energy gap E_g^{cont}:

$$E_g^{cont} = E_c - E_v = E_g + \Delta E_c^{hyd} - \Delta E_{v,moy}^{hyd} - max\left(\Delta E_{hh}^{cisa}, \Delta E_{lh}^{cisa}\right) \quad (15)$$

For a layer subjected to a compressive stress of the energy band of heavy holes is directly above the energy band of light holes and it has:

$$max\left(\Delta E_{hh}^{cisa}, \Delta E_{lh}^{cisa}\right) = \Delta E_{lh}^{cisa} \quad (16)$$

So equation (15) becomes for layer compression

$$E_g^{cont,com} = E_g + \Delta E_c^{hyd} - \Delta E_{v,moy}^{hyd} - \Delta E_{hh}^{cisa} \quad (17)$$

and for a stained layer:

$$E_g^{cont,ten} = E_g + \Delta E_c^{hyd} - \Delta E_{v,moy}^{hyd} - \Delta E_{lh}^{cisa} \quad (18)$$

Determining the forced energy gap requires knowledge of the unstressed $E_g$and $\Delta_0$spin-orbit of the relaxed layer, the elastic constants $C_{ij}$of the layer, the hydrostatic deformation potentials $a_c$and a_v; b is the tetragonal deformation potential. These parameters are listed in appendix for binary II-VI compounds. In cases where the strain layer is a ternary $A_{(1-x)}B_xC$, these parameters can be determined by linear interpolation, except for energy, E_g and $\Delta_0$which are determined by the following expression:

$$E_{A_{(1-x)}B_xC} = (1-x)E_{AC} + xE_{BC} - x(1-x)C_{AC-BC} \quad (19)$$

C_{AC-BC} is the Boeing constant.

2.2 Absorption coefficient

A photon of E energy is absorbed by the material and induces electronic transitions between different states. Thus, for each photon absorbed, a transfer of energy E is the incident light beam directed towards the absorbing medium. For a material having a direct gap, absorption is very likely that this electronic transition is associated with only two particles: electron -photon. The photon conserves energy during the transition between the valence band and the conduction band [9].This interaction between photon and semiconductor leads to an essential characteristic of the material in the field of photovoltaics: the absorption coefficient [10].The absorption coefficient determines the thickness of a material from which a particular wavelength can penetrate before it is absorbed. We classify materials as opaque, translucent and transparent in accordance with their absorption capability [11]. In the case of our alloy $Cd_{1-x}Zn_xTe$ the gap is direct type and results in the relation giving α as a function of hv the form:

$$\alpha(hv) = A^*(hv - \frac{E_g}{q})^{1/2} \quad (20)$$

where A : constant ($2.2 * 10^5$).

2.3 Mechanisms of conduction in an illuminated cell

The solar cells are characterized by their common tension curves under illumination J (V), the latter allows us to calculate the maximum power delivered by the solar cell conversion efficiency and

$$J(V) = J_{Ph} - J_{dif} - J_{Te} \quad (21)$$

with :

J_{ph} : generated photo-current density.
J_{Te} : thermionic current density.
J_{dif} : diffusion current density.
In the photovoltaic cell, there are two opposing currents, the illumination current (photocurrent I_{ph}) and a diode current called dark currentI_{obs}, resulting in polarization of the component. The resulting current I (V) is [12]:

$$I(V) = I_{obs}(V) - I_{ph} \quad (22)$$

with

$$I_{obs}(V) = I_s\left(e^{\left(\frac{qV}{nkT}\right)} - 1\right) \quad (23)$$

$$I_{ph} = q \times \Phi\left[1 - \frac{e^{-\alpha w}}{1 + \alpha w}\right] \times A \quad (24)$$

where:

*q:*electron charge (q=1.6 x 10^{-19}C).

*V:*voltage across the junction.

k: Boltzmann constant ($k = 1.38\,X10^{-23} J.K^{-1}$).

Φ : flux of incident illumination.

T: temperature (K).

A: area of the PV cell.

I_s is the saturation current of the diode, n is the ideality factor of the diode, depending on the quality of the junction (equal to 1 if the diode is ideal and equal to 2 if the diode is real) .).

3. Results and Discussion

The figure.1 shows the variation of the lattice mismatch as a function of the concentration of zinc. It is observed that the lattice mismatch is positive ($\varepsilon > 0$), whatever the value of the concentration of Zn, it indicates that a tensile stress. We also observe a slight mismatch ($\varepsilon \leq 2$) is obtained for the ternary ($CdZnTe$) when we apply low concentrations of Zn varying between 0 and 30%. Figure.2 shows the variation of the energy gap of the structure $Cd_{(1-x)}Zn_xTe$ /$CdTe$ depending on the composition of Zn. We noticed that the Gap of heavy holes is always higher than its light holes because the ternary stressed extensively. The effect of energy E_{Ph} and Zinc on the absorption coefficient of $Cd_{(1-x)}Zn_xTe/CdTe$ is shown in figure.3. This graph can be divided into three parts: In the first part of the curve we have an absorption coefficient equal to zero ($\alpha = 0$) because the energy E_{Ph} is less than the band gap energy of $Cd_{(1-x)}Zn_xTe$, so there is no absorption. In result there is a very fast increase of the absorption coefficient because $E_{Ph}$is greater than the band gap of this structure. The last part there is a saturation of the absorption coefficient with increasing E_{Ph} because in this case all the electrons of the valence band are excited by this high incident energy. It was found that the absorption is highest for a lattice mismatching less than 2% which corresponds to a concentration $x \leq 30\%$.The figure.4 represents the variation of the characteristic of the current density J voltage (V) of the solar cell according to the concentration of Zn. Increasing the concentration of zinc decreases J_{cc} and open circuit voltage. Thus, for low concentration of x,the current density can reach values around 70 mA/cm^2. On figure.5, we plot the evolution of the power function of the bias voltage for several concentrations of Zinc. We noticed that the power delivered by the cell decreases with increase in the concentration of zinc and is explained by the degradation of the current-voltage characteristic. Therefore, the power is maximal for a lattice detuning below 2%. The table.1 shows the effect of the concentration of zinc concentration and lattice mismatch on the open circuit voltage, form factor and performance.

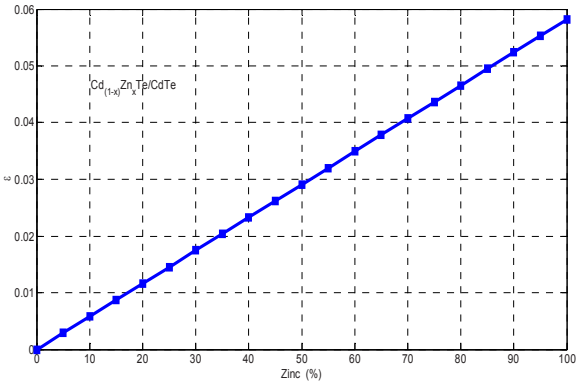

Fig. 1variation in lattice mismatches as a function of the concentration of zinc in the $Cd_{(1-x)}Zn_xTe/CdTe$ structure

.

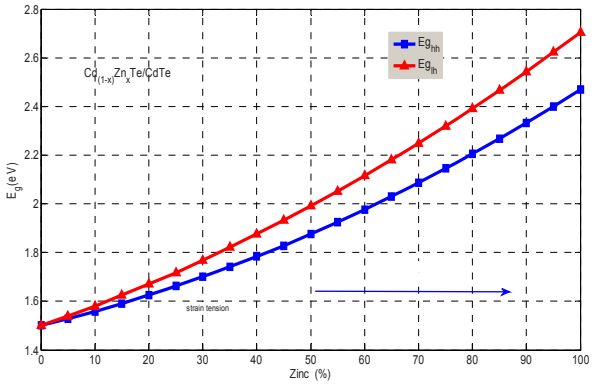

Fig. 2 variation of the energy band gap for strained structure $Cd_{(1-x)}Zn_xTe$ /$CdTe$ versus Zinc concentration (x)

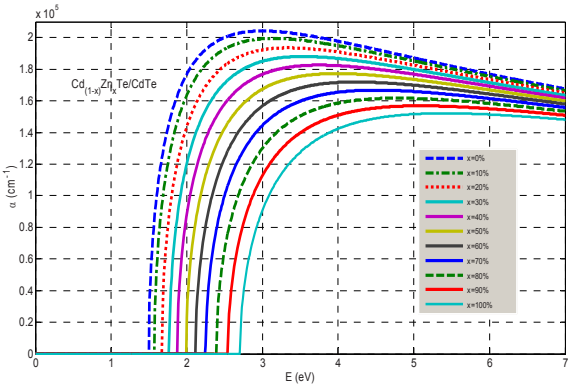

Fig. 3 variation of the absorption coefficient of the $Cd_{(1-x)}Zn_xTe/CdTe$ structure as a function of incident photon energy for various zinc concentrations.

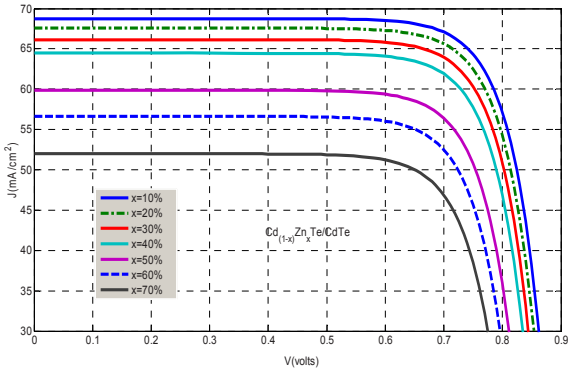

Figure.4 current-voltage characteristics for several concentrations of Zinc (x).

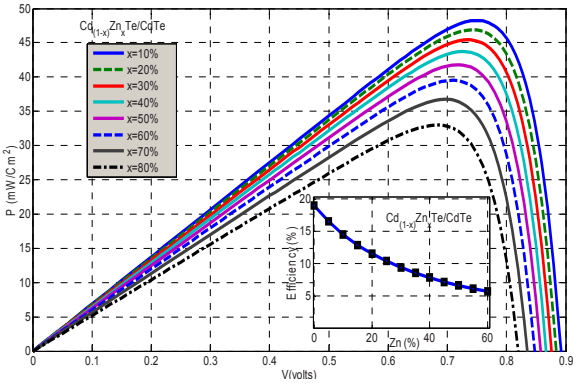

*Fig. 5*power delivered by the cell for several concentrations of Zinc (x).

Table.1 effeciency and fill factor variation with the stress and strain on the basis of the concentration of zinc.

x(%)	ε(%)	V_{co}(V)	FF(%)	η(%)
0	0	0.26	86	18.99
5	0.29	0.30	75	16.52
10	0.5	0.34	65	14.56
20	1.2	0.43	50	12.89
30	1.7	0.53	40	9.38

4. Conclusion

In this work, we studied photovoltaic cell based on II-VI semiconductor material by using $Cd_{1-x}Zn_xTe/Cd$ structure. The ternary material $Cd_{1-x}Zn_xTe$ crystallizes in the zinc blende structure. Its band structure allows vertical radiative transitions between the valence band and the conduction band as it is a material whose Band Gap range varies from 1.50-2.26eV. Our study shows that the change in the gap of $Cd_{1-x}Zn_xTe$ structure increases relatively to the concentration of Zinc. It does not absorb as much of the solar spectrum, but for structure with Zinc concentrations $x \leq 30\%$, illumination absorption is maximal. The epitaxial alloy $Cd_{1-x}Zn_xTe/CdTe$ is subjected to tensile strain. The simulation parameters of the solar cell based on the alloy of zinc have achieved conversion efficiency equal to 19%. To obtain high efficiency solar cells, there is a tradeoff between the strain (ε) and the concentration of Zinc $x(\%)$.

References

[1] Bailly, L., ‘’ Flexible organic photovoltaic cells with large surface", University of Bordeaux I, (2010).
[2] G. Lampel. “Nuclear dynamic polarization by optical electronic saturation and optical pumping in semiconductors”.Phys. Rev. Lett., 20(10):491–493, (1968).
[3] Bordel, D., “Development of New Substrates”, central school of Lyon (2007)
[4] GowriSivaraman, ”Characterization of cadmium zinc telluride solar cells”, Master thesis (supervisor: C. Ferekides), University of South Florida, November (2003)
[5] S. Adachi, “Optical constants of crystalline and amorphous semiconductors”, Kluwer Academic Publishers, Boston, (1999)
[6] S. Adachi, T. Kimura, “Optical constants of $Zn_{1-x}Cd_xTe$ ternary alloys: experiment and modeling”, Japanese Journal of Applied Physics, 32, 3496-3501, (1993)
[7] Mathieu, H.,”Physics of semiconductors and electronic components”, Masson, Paris, (1996).
[8] C.G. Van de Walle “Band lineups and deformation potentials in the model-solid theory” Physical review B, pp. 1871-1883, (1989)
[9] W. Schockley and J. Bardeen “deformation potentials and mobility in non-polar crystals” Phys. Rev. 77, p. 407, (1950)
[10] A.Iller, G. Karczewski, G. Kolmhofer, E. Eusakowsk, H. Sitter, “AES Investigation of Chemical Treatment Effect On CdTe And CdZnTe Surfaces”, Crystal Research Technology, 33, pp.401-409,(1998).
[11] S. Adachi, T. Kimura, ‘Refractive index dispersion of Zn1-xCdxTe ternary alloys’, Japanese Journal of Applied Physics, 32, 3866-3867, (1993)
[12] Nowshad Amin, Kamaruzzaman Sopian, “Makoto KonagaiNumerical modeling of CdS/CdTe and CdS/CdTe/ZnTesolarcells as a function of CdTe thickness” Volume 91, Issue 13, 15 1202–1208 (2007),